Genes & Diseases 8 (2021) 882–890

Available online at www.sciencedirect.com

ScienceDirect

journal homepage: http://ees.elsevier.com/gendis/default.asp

FULL LENGTH ARTICLE

CMTM3 suppresses bone formation and osteogenic differentiation of mesenchymal stem cells through inhibiting Erk1/2 and RUNX2 pathways

Dongwei Fan [a,b], Daoyang Fan [a,b], Wanqiong Yuan [a,b,*]

[a] *Department of Orthopedics, Peking University Third Hospital, 49 North Garden Rd., Haidian District, Beijing, 100191, PR China*
[b] *Beijing Key Laboratory of Spinal Disease, 49 North Garden Rd., Haidian District, Beijing, 100191, PR China*

Received 26 September 2020; received in revised form 15 November 2020; accepted 9 December 2020
Available online 17 December 2020

KEYWORDS
CMTM3;
Erk1/2;
hBMSCs;
Osteoporosis;
RUNX2

Abstract Osteoporosis, fracture, large-scale craniofacial defects and osteonecrosis are hot topics and are still underdiagnosed and undertreated in the clinic. It is urgent to understand the molecular mechanisms corresponding to the regulation of bone formation. CMTM3 (CKLF-like MARVEL transmembrane domain containing 3) connects the classic chemokine to the transmembrane 4 superfamily and plays an important role in intracellular vesicles transport, EGF receptor function maintenance and cancer development. However, its expression and function in bone remain unclear. In this paper, we found that the bone volume/total volume, trabecular number, trabecular thickness and bone surface area/bone volume of *Cmtm3* KO mice increased significantly, and trabecular separation and trabecular pattern factor decreased in *Cmtm3* KO mice compared with WT mice by microcomputed tomography. Moreover, the bone mineral content, bone mineral density, ultimate force and stiffness were also increased in *Cmtm3* KO mice. Using *in vitro* analysis, we showed that CMTM3 expression decreases during the differentiation of hBMSCs to osteoblasts. Knockdown of CMTM3 promoted ALP and mineralization of hBMSCs and facilitated osteoblastic differentiation with increasing RUNX2 expression. However, overexpression of CMTM3 got the opposite results. These results proved that CMTM3 was essential for osteogenic differentiation. In addition, knockdown of CMTM3 enhanced p-Erk1/2, but had no significant effect on p-Akt or p-STAT3 in hBMSCs and MC3T3-E1 cells. Taken together, our results indicated that Erk1/2 and RUNX2 pathways mediated by CMTM3 were involved in the process of osteogenic differentiation, and CMTM3 might be a new potential target in the treatment of bone formation-related disease.

* Corresponding author. Department of Orthopedics, Peking University Third Hospital, 49 North Garden Rd., Haidian District, Beijing, PR China.
E-mail address: yuanwanqiong@bjmu.edu.cn (W. Yuan).
Peer review under responsibility of Chongqing Medical University.

https://doi.org/10.1016/j.gendis.2020.12.003

Introduction

Osteoporosis, non-union after fracture, large-scale craniofacial defects, osteonecrosis, and periodontal diseases are hot topics in the clinic.[1,2] However, these diseases are still underdiagnosed and undertreated and only a few strategies have been translated into clinical practice.[3] One of the main challenges lies in the limited understanding of the cellular and molecular mechanisms corresponding to the promotion of bone formation.[4] In particular, the regulation of the development and differentiation of mesenchymal stem cells into osteoblasts is essential for improving the effectiveness of bone-related disease treatments.[5]

The process of bone formation begins with the regulation of osteoblast differentiation with mesenchymal stem cells (MSCs).[6] First, early differentiation of stem cells into osteoblast progenitor cells induces the differentiation of these osteoblast progenitor cells into immature osteoblasts. Second, these underdeveloped immature osteoblasts commit to the differentiation of mature osteoblasts.[7] MSCs are mainly located in the bone marrow stroma, and can differentiate into mesenchymal lineages, such as fibroblasts, chondrocytes, and bone marrow stromal cells.[8] Many markers are produced during the differentiation, such as alkaline phosphatase (ALP),[9] collagen type I,[10] osteopontin[11] and osteocalcin[12] and the osteogenic transcription factor RUNX2.[13,14] This process leads to the formation of an organic matrix that will be mineralized outside the cells.

CMTM3 (CKLF-like MARVEL transmembrane domain-containing family 3), formerly known as chemokine-like factor super family (CKLFSF) 3, is a member of the CMTM family, which was first reported by our previous research group in 2003.[15,16] In humans, the family includes nine genes, namely *chemokine-like factor (CKLF)* and *CMTM1-8 (CKLF-like MARVEL transmembrane domain-containing member 1–8, CKLFSF1-8)*.[17] The CMTM family plays important roles in the immune system and the male reproductive system, and is involved in the occurrence and development of cancers.[18–21] It has been reported that CMTM3 was silenced by CpG methylation in multiple cancer types,[22] and we found that CMTM3 suppressed gastric cancer by promoting EGFR degradation and inhibiting EGFR/STAT3 signaling pathway via promoting Rab5 activation.[23–25]

The results of previous mass spectrometry analysis showed that CMTM3 is not only related to membrane receptor aggregation, internalization and intracellular material transport, but is also closely related to the Erk1/2 signaling pathway which plays important roles in osteoblast differentiation. In this study, we determined that *Cmtm3* knockout (KO) mice had higher bone density and bone strength than the wild-type (WT) mice using micro-computed tomography (micro-CT), dual energy X-ray absorptiometry (DXA), and biomechanical testing. *In vitro* experiments also found that CMTM3 is closely related to osteoblast differentiation. Knockdown of CMTM3 promoted the differentiation of human bone marrow stromal cells (hBMSCs) to osteoblasts, and overexpression of CMTM3 inhibited hBMSCs differentiation. Moreover, Erk1/2 and RUNX2 were involved in the differentiation of osteoblasts regulated by CMTM3 in hBMSCs and MC3T3-E1 cells. In general, deficiency of CMTM3 promoted osteogenic differentiation by promoting the expression of RUNX2 and activation of the Erk1/2 signaling pathway.

Material and methods

Animals and cell sample collection

Twelve-week-old female WT C57BL/6 and *Cmtm3* KO mice (background strain, C57BL/6) were obtained from Professor Han (Department of Immunology, Peking University Health Science Center, Beijing, China). The *Cmtm3* KO mice were created according to the Crisper Cas9 method. All mice were housed individually in standard cages with a 12:12 h light/dark cycle and room temperature maintained at 21 ± 1 °C. The lumbar spine, femur and tibia were harvested for micro-CT, DXA assessment and biomechanical testing by wrapping the specimens in saline-soaked gauze and freezing at −80 °C.

Micro-CT scan analysis

The lumbar spine, femur and tibia of WT and *Cmtm3* KO mice were scanned by micro-CT (Inveon, Siemens, Erlangen, Germany) at an effective pixel size of 8.82 μm, a current of 500 μA, a voltage of 80 kV, and an exposure time of 1500 ms in each of the 360 rotational steps. The images were then reconstructed using the Inveon Acquisition Workplace (Siemens, Erlangen, Germany). We counted 150 axial slices distal and proximal to the fracture line, approximately 2.65 mm. According to the guidelines set by the American Society for Bone and Mineral Research, we selected the second ROI in the trabecular region (150 axial slices, approximately 1.3 mm distal to the proximal epiphyseal plate), and the bone volume/total volume (BV/TV), bone surface area/bone volume (BS/BV), trabecular thickness (Tb.Th), trabecular number (Tb.N), trabecular separation (Tb.Sp) and trabecular pattern factor (Tb.Pf) were calculated.

Dual energy X-ray absorptiometry (DXA) assessment

Bone mineral content (BMC) and bone mineral density (BMD) were measured by high-resolution DXA (Ultra Focus DXA, Faxitron). The manufacturer's recommended

calibration procedure was performed daily before scanning. The BMC (*g*) was analyzed and the BMD (g/cm^2) was calculated by the software as the ratio between BMC and bone area.

Biomechanical testing

To evaluate the mechanical properties of tibiae and femurs, a three-point bending test was performed using a mechanical testing system (MTS Landmark Systems, Eden Prairie, MN) with a load cell of 100 N. Before mechanical testing, the samples were thawed to room temperature and then kept moist with saline-soaked gauze. Then, tibiae were placed with their posterior side facing down between two supports with a 10-mm span and femurs were placed directly under the middle anvil with an 8-mm working gauge length. A preload of 0.5 N was applied at the middle point of the bone. A compressive force was applied to the bone at a speed of 1 mm per minute. The ultimate force (the force applied at the failure point) and stiffness were calculated on the basis of the resulting force—displacement curves.

H&E staining

Right femurs were isolated and fixed in 4% paraformaldehyde for 24 h, decalcified in 12.5% EDTA (pH 7.0) for 2 weeks, and embedded in paraffin. Longitudinal sections with a thickness of 5 μm were cut and stained with H&E staining in accordance with the manufacturer's protocols.

Cell culture and cell differentiation

hBMSCs were obtained from the iCell Bioscience Inc (Shanghai, China) and cultured in high glucose DMEM (Invitrogen, Carlsbad, CA, USA) supplemented with 10% fetal bovine serum (FBS) and 1% penicillin—streptomycin. The mouse preosteoblastic cell line MC3T3-E1 was obtained from the Cell Bank of the Chinese Academy of Science (Shanghai, China) and was cultured in α-minimum essential medium (MEM) (Invitrogen, Carlsbad, CA, USA) supplemented with 10% FBS and 1% penicillin—streptomycin. These cells were incubated in 5% CO_2 at 37 °C.

To induce cell differentiation, the cells were seeded into plates at a density of 5×10^5 cells/mL. When reached 80% confluence, cells were transferred to differentiation medium (DM) containing 10% FBS with 10—8 M dexamethasone (Sigma—Aldrich), 50 μg/mL ascorbic acid (Sigma—Aldrich) and 5 mM β-glycerol phosphate (Sigma—Aldrich). Fresh medium was applied every three days.

Real-time reverse transcription PCR

Briefly, total RNA was extracted from cells using TRIzol reagent (Life Technologies, Inc.) according to standard protocols. Amplifications were performed using a SYBR Green PCR Master Mix Kit (Biosystems, USA) in a total volume of 20 μL. Template cDNA was denatured at 95 °C for 10 min followed by 40 cycles of 95 °C for 15 s and 60 °C for 1 min. Real-time PCR was performed using the following primers, CMTM3-F: 5′ CCTGATCTTTAACGACGTGGC-3′, CMTM3-R: 5′-TTCTTCTGTCTTGTGGGCTGTG-3″ and GAPDH-F: 5′-GGAAGCTTGTCATCAATGGAAATC-3′, GAPDH-R: 5′- TGATGACCCTTTTGGCTCCC-3'. GAPDH was the internal control.

Western blot

Western blot was performed as previously described.[25] Equal amounts of proteins were separated by SDS-PAGE electrophoresis and electro-transferred onto a polyvinylidene difluoride membrane (Immobilon, Millipore). After blocking in TBS-T plus 5% non-fat milk for 1 h, membranes were incubated with primary antibodies against Erk1/2 and phosphor-Erk1/2 (Thr202/Tyr204), Akt (pan) and phosphor-Akt (Ser473), STAT3 and phosphor-STAT3 (Tyr705), RUNX2 (CST, MA, USA) and CMTM3 (Abcam, Cambridge, UK) at 4 °C overnight. Then, membranes were incubated with secondary antibodies and signals were detected by LAS500 (GE, New York, NY).

Adenovirus construction

The construction, generation and purification of the ad5-null (vector-containing adenovirus, defined as MOCK) and ad5-CMTM3 vectors were provided by Hanbioco. Ltd (Shanghai, China). The empty adenovirus was used in parallel as a negative control and adenoviruses were infected with a multiplicity of infection (MOI) of 100.

siRNA transfection

To knock down endogenous CMTM3, the following target sequences were constructed in a small interfering RNA (siRNA): si-CMTM3-1#, 5′-GCCCUCAUCUACUUUGCUATT-3′, si-CMTM3-2#, 5′-GCAACUGAUUUCUACCUGATT-3'. A scrambled siRNA (Scr) was used as a negative control (sequence: 5′-UUCUCCGAACGUGUCACGUTT-3′). The siRNAs and the positive control siRNA FAM were purchased commercially (Gene Pharma Inc., Shanghai, China). Cells were transfected with siRNA two days later at a final concentration of 50 nM using Lipofectamine 3000 transfection reagent (Life Technologies, Carlsbad, CA) for subsequent experiments. The suppression efficiency of CMTM3 was analyzed by Western blot two days post transfection.

Alkaline phosphatase (ALP) activity assay

Seven days after treatment, cells were washed three times with phosphate-buffered saline (PBS), fixed in 4% paraformaldehyde for 5 min at room temperature, and then washed three times with PBS again. ALP staining was carried out according to the manufacturer's instructions (Solarbio, Beijing, China).

Alizarin red staining

To examine the mineralization of hBMSCs, cells were cultured for three weeks with DM and then mineralized to form opaque calcified nodules. The cells were washed three times with Ca^{2+}-free PBS, fixed with 4%

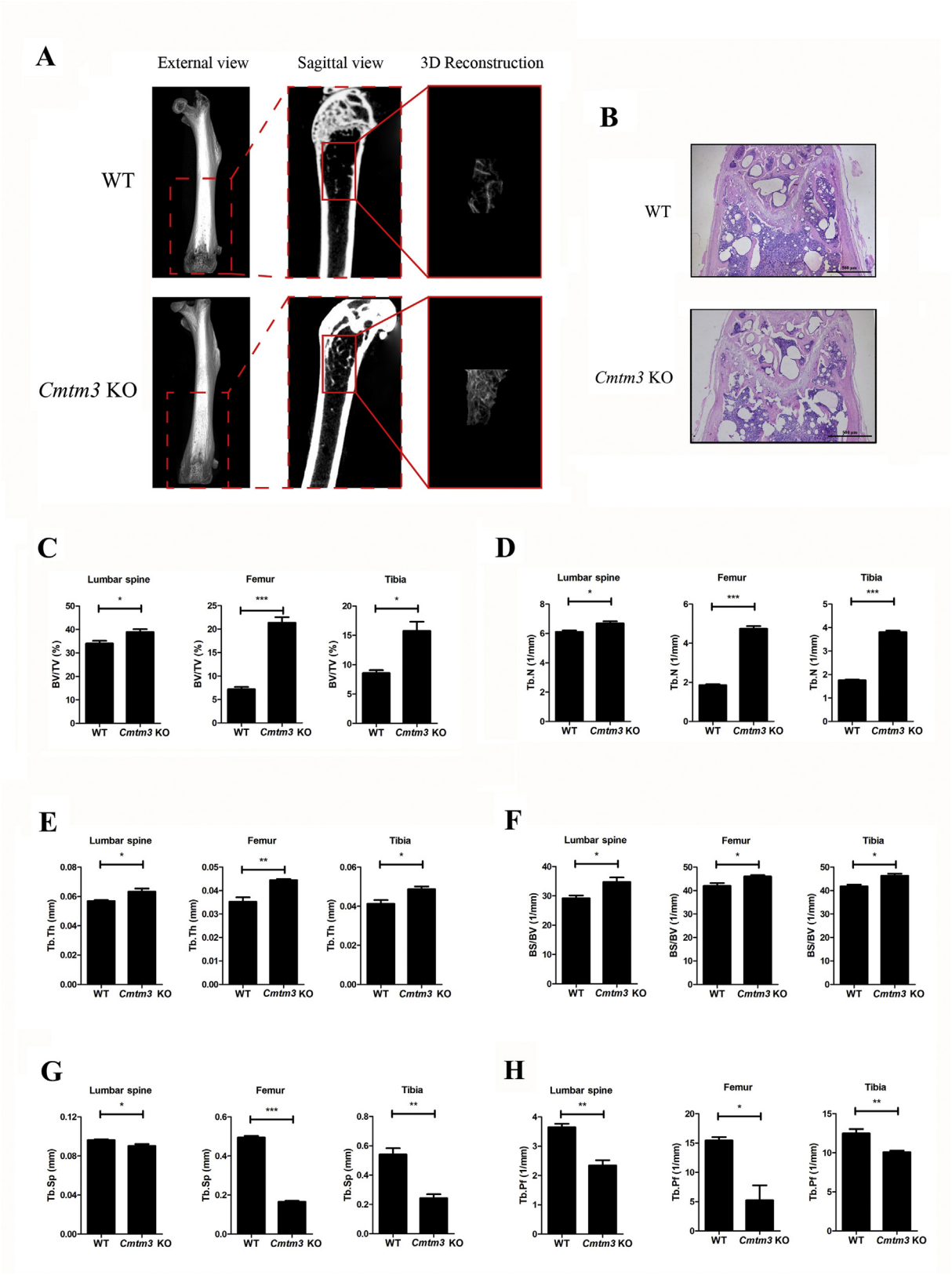

Figure 1 Bone microstructure is improved in *Cmtm3* KO mice ($n = 6$). **(A)** Microstructure images of femurs in female-WT and *Cmtm3* KO mice. **(B)** H&E staining of the femur from female-WT and *Cmtm3* KO mice. **(C)** BV/TV (%), **(D)** Tb.N (1/mm), **(E)** Tb.Th (mm), **(F)** BS/BV (1/mm), **(G)** Tb.Sp (mm) and **(H)** Tb. Pf (1/mm) were calculated. Data were presented as the mean ± SD (*$P < 0.05$, **$P < 0.01$, ***$P < 0.001$).

paraformaldehyde for 15 min, washed three times with PBS again and stained with 0.1% alizarin red solution for 30 min at room temperature. Finally, they were rinsed with PBS and observed under an inverted light microscope.

Statistical analysis

All data are expressed as the mean ± SD and were checked for normality. Statistical analysis was carried out with Student's *t*-test with Prism 5.0 (GraphPad Software, San Diego, CA, USA). Differences were considered significant at $P < 0.05$ (two-sided).

Results

Knockout of *Cmtm3* promotes bone formation *in vivo*

Micro-CT was used for microstructural analysis of the lumbar spine, femur and tibia in female-WT and female-*Cmtm3* KO mice. Micro-CT images revealed that the microstructure of the *Cmtm3* KO mice obviously improved compared with the WT mice (Fig. 1A). H&E staining showed that more trabecular bones were observed on female-*Cmtm3* KO mice compared with the WT mice (Fig. 1B). BV/TV (Fig. 1C), Tb.N (Fig. 1D), Tb.Th (Fig. 1E) and BS/BV (Fig. 1F) of the lumbar spine, femur and tibia significantly increased in *Cmtm3* KO mice. However, Tb.Sp (Fig. 1G) and Tb.Pf (Fig. 1H) of the lumbar spine, femur and tibia decreased in *Cmtm3* KO mice in comparison with WT mice. The above parameters were also analyzed in male-WT and male-*Cmtm3* KO mice and we got consistent results (Fig. S1). Taken together, we proposed that knockout of *Cmtm3* promoted bone formation.

Knockout of *Cmtm3* increases bone quality

Further, the BMCs (Fig. 2A—C) and BMDs (Fig. 2D—F) of the lumbar spine, tibia and femur in female-*Cmtm3* KO mice increased compared with the those in female-WT mice by DXA. In addition, a three-point bending test of the femur and tibia was performed and we observed the ultimate force and stiffness also increased in both the femur and tibia of the female-*Cmtm3* KO mice (Fig. 2G—J) and male-*Cmtm3* KO mice (Fig. S2A-D) compared with the age and gender-matched WT mice.

Knockdown of CMTM3 promotes the osteogenic differentiation

To clarify the roles of CMTM3 in osteoblast differentiation *in vitro*, CMTM3 expression was analyzed during the differentiation progression of hBMSCs. We collected hBMSCs cultured in DM for 9, 12, 15 and 18 days, respectively, and found that the longer the cells were cultured in DM, the less CMTM3 was expressed (Fig. 3A and B). Then, CMTM3 was silenced by siRNA or restored by adenovirus in hBMSCs, and ALP staining and Alizarin staining assays were carried out. As shown in Fig. 3C, knockdown of CMTM3 exhibited significantly higher ALP activity and calcification than the si-Scr group cells in hBMSCs. Consistently, restoration of CMTM3 reduced ALP activity in hBMSCs (Fig. 3D). Meanwhile, we performed Alizarin staining assay to explore the role of CMTM3 in the calcification of hBMSCs and found that silencing CMTM3 increased the calcified nodules of hBMSCs, while overexpression of CMTM3 revealed the opposite results (Fig. 3E and F). Therefore, we suggested that CMTM3 suppressed osteogenesis *in vitro*.

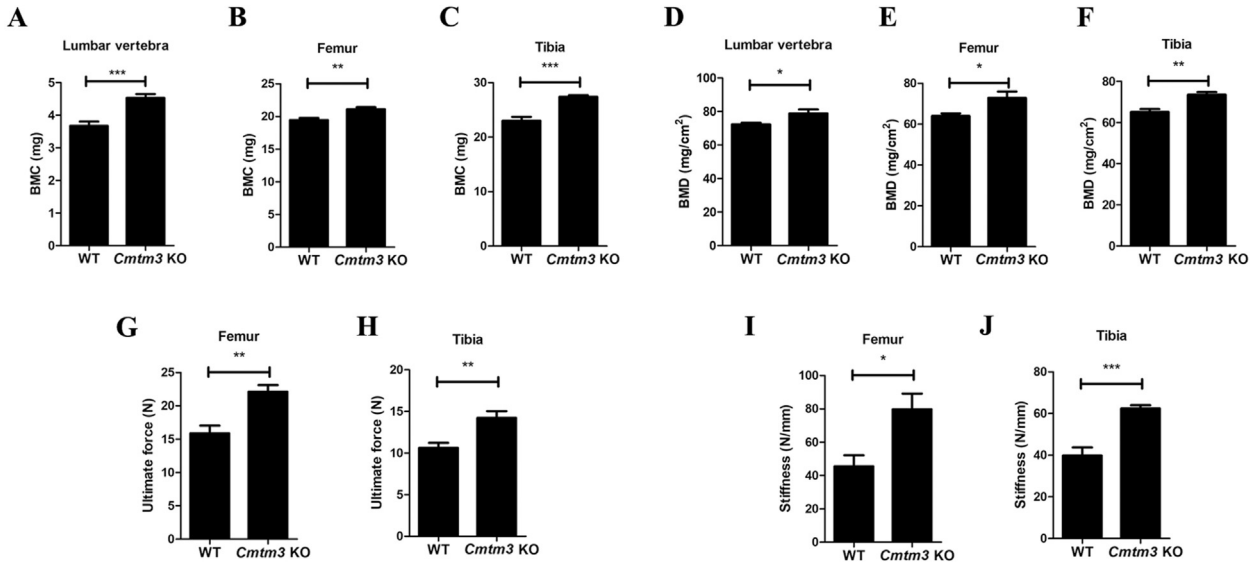

Figure 2 Knockout of *Cmtm3* increases the bone quality of the lumbar spine, tibia and femur ($n = 6$). **(A—C)** BMCs (mg) of the lumbar spine, femur and tibia were analyzed by DAX. **(D—F)** BMDs (mg/cm^2) of the lumbar spine, femur and tibia were analyzed by DAX. **(G—H)** The ultimate force (N) values of the femur and tibia were analyzed by MTS Landmark Systems. **(J—L)** Stiffness (N/mm) of the femur and tibia was analyzed by MTS Landmark Systems. Data were presented as the mean ± s.d (*$P < 0.05$, **$P < 0.01$, ***$P < 0.001$).

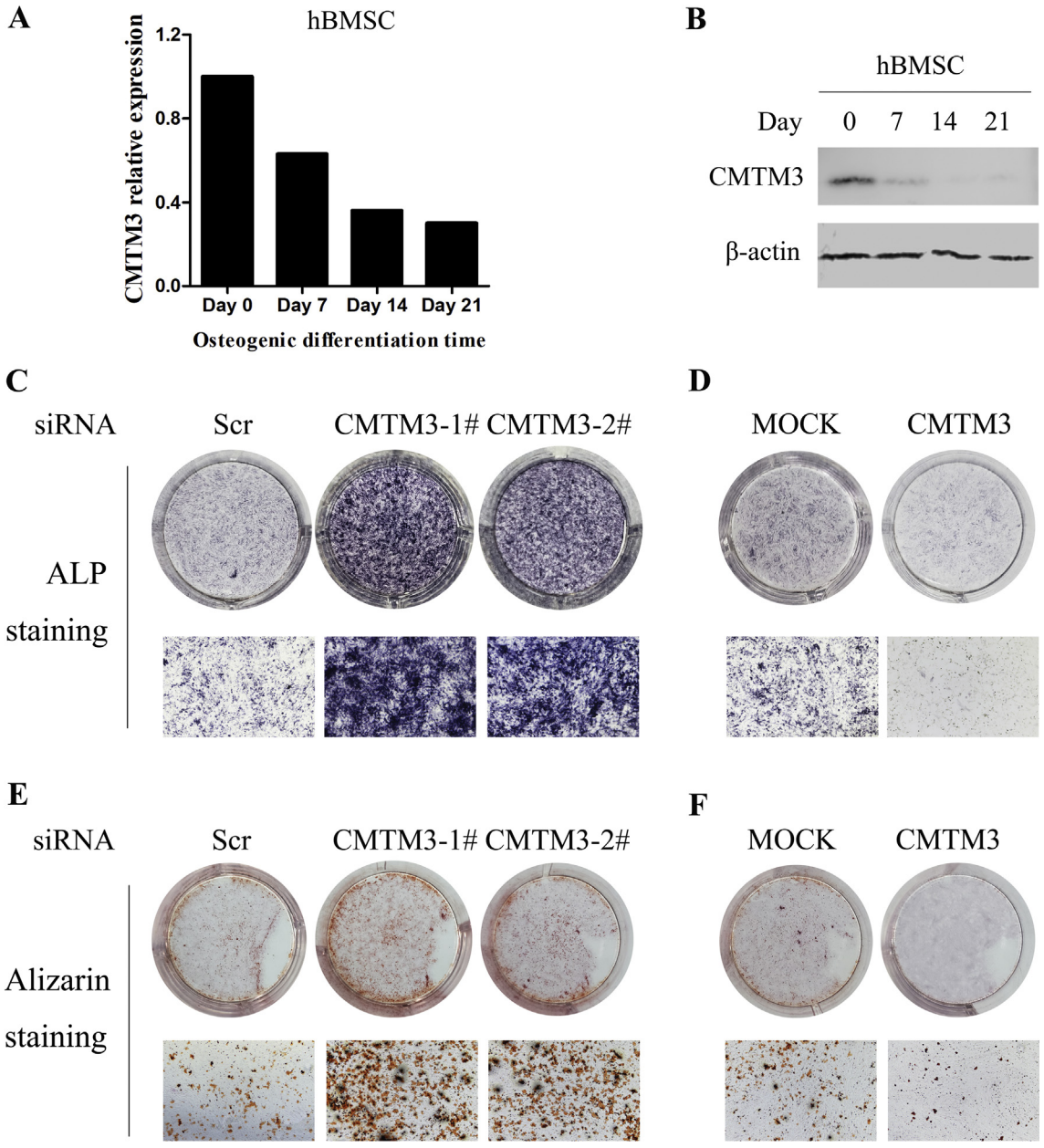

Figure 3 Silencing CMTM3 promotes the osteogenic differentiation *in vitro*. **(A)** The expression of CMTM3 was analyzed by real-time PCR in hBMSCs. All samples subjected to real-time PCR were run in triplicate. Representative data were shown as the average number from one independent experiment. **(B)** The expression of CMTM3 was analyzed by Western blot in hBMSCs. 100 μg of total protein was loaded. **(C)** ALP staining in the CMTM3 knockdown system (top, visual inspection, bottom, photomicrograph, 40× magnification). **(D)** ALP staining in the CMTM3 restored system (top, visual inspection, bottom, photomicrograph, 40×). **(E)** Alizarin staining assay in the CMTM3 knockdown system (top, visual inspection, bottom, photomicrograph, 40×magnification). **(F)** Alizarin staining assay in CMTM3 restored system (up, visual inspection, down, photomicrograph, 40×). Data were representative of three independent experiments.

CMTM3 suppresses osteogenic differentiation via the Erk/RUNX2 pathway

CMTM3 is a conserved protein with 88% homology between humans and mice. We further expatiated the mechanism of CMTM3 in regulating osteogenic differentiation in hBMSCs and mouse preosteoblastic MC3T3-E1 cells and found that knockdown of CMTM3 upregulated the expression of RUNX2, an osteoblast marker and restored CMTM3 downregulated RUNX2 expression in hBMSCs and MC3T3-E1 cells (Fig. 4A–D). To gain insight into the mechanism of CMTM3 in suppressing osteogenic differentiation, the related signaling pathways, including STAT3, Akt, and Erk1/2 were analyzed. The levels of total and phosphorylated STAT3 (Tyr705), Akt (Ser473) and Erk1/2 (Thr202/Tyr204) were detected in hBMSCs and MC3T3-E1 cells in CMTM3 restored and knockdown systems. No significant difference was observed in the levels of p-Akt, and p-STAT3 in these cells,

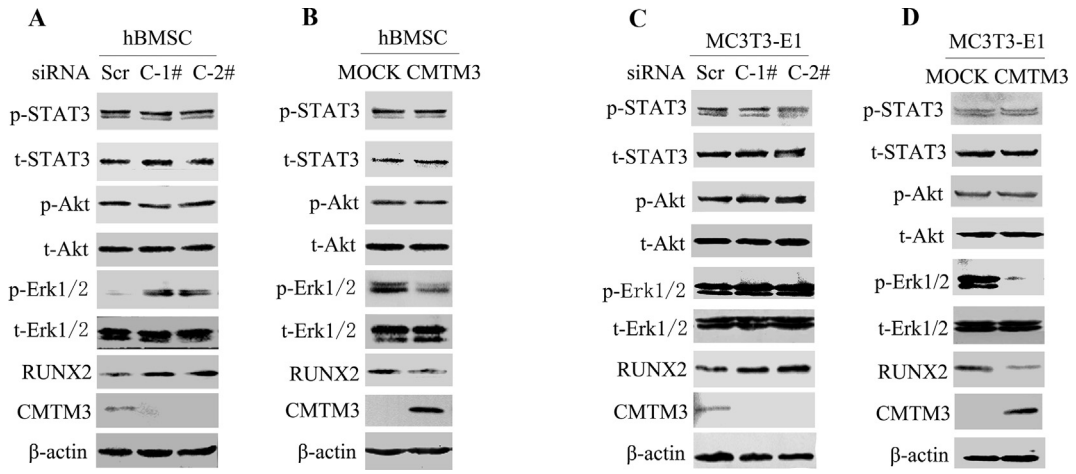

Figure 4 CMTM3 suppresses osteogenic differentiation though the Erk/RUNX2 pathway. **(A)** The expression of RUNX2 and phosphorylated and total STAT3, Akt and Erk1/2 were analyzed in CMTM3 knockdown hBMSCs. **(B)** The expression of RUNX2 and the phosphorylated and total STAT3, Akt and Erk1/2 were analyzed in CMTM3 restored hBMSC (MOI: 100). **(C)** The expression of RUNX2 and the phosphorylated and total STAT3, Akt and Erk1/2 were analyzed in CMTM3 knockdown MC3T3-E1 cells. **(D)** The expression of RUNX2 and phosphorylated and total STAT3, Akt and Erk1/2 were analyzed in CMTM3 restored MC3T3-E1 cells (MOI: 100). To detect CMTM3, 100 μg of total protein was loaded in the CMTM3 knockdown system and 40 μg total protein was loaded in the CMTM3 restored system.

but p-Erk1/2 was markedly augmented in CMTM3 knockdown cells and decreased in CMTM3 overexpressing cells (Fig. 4A—D). These data demonstrated that CMTM3 downregulated RUNX2 expression and hindered the phosphorylation of Erk1/2 during osteogenic differentiation.

Discussion

Fractures and subsequent bone healing processes are almost always accompanied by endogenous and differentiated ability of transplanted stem cells [26]. Due to their self-renewal and multiple differentiation capabilities, hBMSCs are currently considered to be an important tool for cell-based bone tissue engineering treatment of bone healing[27,28]. Therefore, it is of clinical significance to reveal the mechanism regulating the differentiation of hBMSCs into osteoblasts. CMTM3 plays a vital role in various biological processes in different tissues.[29,30] In this study, we found that Cmtm3 caused abnormal development of mouse bone and proved that CMTM3 played an important role in the MSC osteogenesis process. Silencing CMTM3 can significantly increase the osteogenic potential of hBMSCs *in vitro*, indicating that CMTM3 has an inhibitory effect on bone formation. In summary, CMTM3 plays an important role in bone development.

To date, CMTM3 has not been reported to be related to osteogenic function. Our data showed for the first time that CMTM3 was endogenously expressed in hBMSCs, which was confirmed by Real-time PCR at the mRNA level and Western blot at the protein level. Moreover, we observed that CMTM3 downregulated the expression of the osteogenic marker RUNX2, indicating that CMTM3 may maintain the undifferentiated state of hBMSCs. After CMTM3 silencing, hBMSCs showed stronger osteogenic differentiation abilities *in vitro* and *in vivo* than the overexpressed groups. At a later time of osteogenic differentiation, we found that knockdown of CMTM3 significantly increased ALP activity and mineralized nodules compared with the control group. ALP positive and mineralized nodules were obviously decreased in CMTM3-restored hBMSCs in comparation with MOCK-hBMSCs. Osteoblast bone formation requires various key transcription factors and signaling pathways, including RUNX2,[31] TAZ,[32] Wnt,[33,34] BMP[35,] MAPK/Erk,[36,37] Akt[38] and STAT3[39] signaling pathways. Among them, the transcription factor RUNX2 plays a vital role in the finalization of hBMSC differentiation into osteoblast lineages. In this study, we investigated the mechanism behind the phenomenon of increased the expression of RUNX2 by silencing CMTM3, which led to osteoblast differentiation of hBMSCs.[40] We tested the phosphorylation of CMTM3-related signaling pathways in CMTM3 knockdown and overexpression systems and our results indicated that CMTM3 knockdown increased the phosphorylation of Erk1/2 and overexpression of CMTM3 suppressed the phosphorylation of Erk1/2. However, no changes were observed in p-STAT3 or p-Akt by knockdown and restoration of CMTM3, strongly supporting the hypothesis that CMTM3 inhibited osteoblast differentiation of hBMSCs through the Erk1/2 signaling pathway.

Overall, our research indicates that CMTM3 plays an endogenous inhibitory role in the process of bone mesenchymal cell osteogenesis. These findings describe the mechanism of CMTM3 silencing in the osteogenic differentiation of hBMSCs and may further help translate these basic findings into future clinical applications.

Conclusions

The findings of this study indicate that *Cmtm3* KO mice show better bone quality than WT mice. Silencing CMTM3 promotes osteoblast differentiation of hBMSCs *in vitro*, tending to drive MSCs into the osteoblast differentiation process through promoting the Erk1/2 and RUNX2 signaling pathways. Therefore, CMTM3 may be a therapeutic target for treating bone diseases such as bone healing, and may

accelerate bone healing treatment in combination with bone biomaterial scaffolds.

Ethics approval and consent to participate

All animal experiments in this research were performed in accordance with currently prescribed guidelines and followed a standard protocol approved by the Biomedical Ethics Committee of Peking University (approval number: A2020165).

Consent for publication

The authors agree with publication of this paper.

Data statement (where applicable)

The datasets used or analyzed during the current study are available from the corresponding author on reasonable request.

Authors contribution

Dongwei Fan: Investigation, data curation, writing-original draft. Daoyang Fan: Data curation and investigation. Wanqiong Yuan: Project administration, funding acquisition, methodology and writing-review & editing. All authors read and approved the final manuscript.

Conflict of Interests

The authors declare that there are no conflicts of interest.

Funding

The authors would like to thank Prof. Wenling Han for insightful suggestions and generously providing *Cmtm3* KO mice at Peking University Health Science Center (Beijing, China). This work was supported by the Key Clinical Projects of Peking University Third Hospital [grant number BYSYZD2019041].

List of abbreviations

ALP	Alkaline phosphatase
BMC	Bone mineral content
BMD	Bone mineral density
BS/BV	Bone surface area/bone volume
BV/TV	Bone volume/total volume
CKLF	Chemokine-like factor
CKLFSF	Chemokine-like factor super family
CMTM	CKLF-like MARVEL transmembrane domain family
DXA	Dual energy X-ray absorptiometry
FBS	Fetal bovine serum
hBMSC	Human bone marrow stromal cells
KO	Knockout
Micro-CT	Microcomputed tomography
MSC	Mesenchymal stem cells
Tb.N	Trabecular number
Tb.Th	Trabecular thickness
Tb.Pf	Trabecular pattern factor
Tb.Sp	Trabecular separation
WT	Wild type

Appendix A. Supplementary data

Supplementary data to this article can be found online at https://doi.org/10.1016/j.gendis.2020.12.003.

References

1. Won Lee G, Thangavelu M, Joung Choi M, et al. Exosome mediated transfer of miRNA-140 promotes enhanced chondrogenic differentiation of bone marrow stem cells for enhanced cartilage repair and regeneration. *J Cell Biochem*. 2020;121(7):3642–3652.
2. Yang TL, Shen H, Liu A, et al. A road map for understanding molecular and genetic determinants of osteoporosis. *Nat Rev Endocrinol*. 2020;16(2):91–103.
3. Khosla S. Personalising osteoporosis treatment for patients at high risk of fracture. *Lancet Diabetes Endocrinol*. 2019;7(10):739–741.
4. Fuggle NR, Curtis EM, Ward KA, Harvey NC, Dennison EM, Cooper C. Fracture prediction, imaging and screening in osteoporosis. *Nat Rev Endocrinol*. 2019;15(9):535–547.
5. Han L, Wang B, Wang R, Gong S, Chen G, Xu W. The shift in the balance between osteoblastogenesis and adipogenesis of mesenchymal stem cells mediated by glucocorticoid receptor. *Stem Cell Res Ther*. 2019;10(1),e377.
6. Knani L, Bartolini D, Kechiche S, et al. Melatonin prevents cadmium-induced bone damage: first evidence on an improved osteogenic/adipogenic differentiation balance of mesenchymal stem cells as underlying mechanism. *J Pineal Res*. 2019;67(3), e12597.
7. Lin Z, He H, Wang M, Liang J. MicroRNA-130a controls bone marrow mesenchymal stem cell differentiation towards the osteoblastic and adipogenic fate. *Cell Prolif*. 2019;52(6), e12688.
8. Baccin C, Al-Sabah J, Velten L, et al. Combined single-cell and spatial transcriptomics reveal the molecular, cellular and spatial bone marrow niche organization. *Nat Cell Biol*. 2020;22(1):38–48.
9. Sterner RM, Kremer KN, Dudakovic A, Westendorf JJ, van Wijnen AJ, Hedin KE. Tissue-nonspecific alkaline phosphatase is required for MC3T3 osteoblast-mediated rotection of acute myeloid leukemia cells from apoptosis. *J Immunol*. 2018;201(3):1086–1096.
10. Uchihashi K, Aoki S, Matsunobu A, Toda S. Osteoblast migration into type I collagen gel and differentiation to osteocyte-like cells within a self-produced mineralized matrix: a novel system for analyzing differentiation from osteoblast to osteocyte. *Bone*. 2013;52(1):102–110.
11. Luo Y, Grötsch B, Hannemann N, et al. Fra-2 expression in osteoblasts regulates systemic inflammation and lung injury through osteopontin. *Mol Cell Biol*. 2018;38(22),e00022-18.
12. Zoch ML, Clemens TL, Riddle RC. New insights into the biology of osteocalcin. *Bone*. 2016;82:42–49.
13. Yang D, Okamura H, Nakashima Y, Haneji T. Histone demethylase Jmjd3 regulates osteoblast differentiation via transcription factors Runx2 and osterix. *J Biol Chem*. 2013;288(47):33530–33541.
14. Wei J, Shimazu J, Makinistoglu MP, et al. Glucose uptake and Runx2 synergize to orchestrate osteoblast differentiation and bone formation. *Cell*. 2015;161(7):1576–1591.

15. Zhong J, Wang Y, Qiu X, et al. Characterization and expression profile of CMTM3/CKLFSF3. *J Biochem Mol Biol*. 2006;39(5):537—545.
16. Han W, Lou Y, Tang J, et al. Molecular cloning and characterization of chemokine-like factor 1 (CKLF1), a novel human cytokine with unique structure and potential chemotactic activity. *Biochem J*. 2001;357(Pt 1):127—135.
17. Han W, Ding P, Xu M, et al. Identification of eight genes encoding chemokine-like factor superfamily members 1-8 (CKLFSF1-8) by in silico cloning and experimental validation. *Genomics*. 2003;81(6):609—617.
18. Li Z, Xie J, Wu J, et al. CMTM3 inhibits human testicular cancer cell growth through inducing cell-cycle arrest and apoptosis. *PLoS One*. 2014;9(2), e88965.
19. Han T, Shu T, Dong S, et al. Chemokine-like factor-like MARVEL transmembrane domain-containing 3 expression is associated with a favorable prognosis in esophageal squamous cell carcinoma. *Oncol Lett*. 2017;13(5):2982—2988.
20. Di Meo S, Airoldi I, Sorrentino C, Zorzoli A, Esposito S, Di Carlo E. Interleukin-30 expression in prostate cancer and its draining lymph nodes correlates with advanced grade and stage. *Clin Cancer Res*. 2014;20(3):585—594.
21. Abe M, Yamashita S, Mori Y, et al. High-risk oral leukoplakia is associated with aberrant promoter methylation of multiple genes. *BMC Cancer*. 2016;16,e350.
22. Wang Y, Li J, Cui Y, et al. CMTM3, located at the critical tumor suppressor locus 16q22.1, is silenced by CpG methylation in carcinomas and inhibits tumor cell growth through inducing apoptosis. *Cancer Res*. 2009;69(12):5194—5201.
23. Su Y, Lin Y, Zhang L, et al. CMTM3 inhibits cell migration and invasion and correlates with favorable prognosis in gastric cancer. *Cancer Sci*. 2014;105(1):26—34.
24. Yuan W, Li T, Mo X, et al. Knockdown of CMTM3 promotes metastasis of gastric cancer via the STAT3/Twist1/EMT signaling pathway. *Oncotarget*. 2016;7(20):29507—29519.
25. Yuan W, Liu B, Wang X, et al. CMTM3 decreases EGFR expression and EGF-mediated tumorigenicity by promoting Rab5 activity in gastric cancer. *Cancer Lett*. 2017;386:77—86.
26. Cheng Z, Li A, Tu CL, et al. Calcium-sensing receptors in chondrocytes and osteoblasts are required for callus maturation and fracture healing in mice. *J Bone Miner Res*. 2020;35(1):143—154.
27. Chen J, Ashames A, Buabeid MA, Fahelelbom KM, Ijaz M, Murtaza G. Nanocomposites drug delivery systems for the healing of bone fractures. *Int J Pharm*. 2020;585,e119477.
28. Zhao SJ, Kong FQ, Jie J, et al. Macrophage MSR1 promotes BMSC osteogenic differentiation and M2-like polarization by activating PI3K/AKT/GSK3beta/beta-catenin pathway. *Theranostics*. 2020;10(1):17—35.
29. Chrifi I, Louzao-Martinez L, Brandt M, et al. CMTM3 (CKLF-Like marvel transmembrane domain 3) mediates angiogenesis by regulating cell surface availability of VE-cadherin in endothelial adherens junctions. *Arterioscler Thromb Vasc Biol*. 2017;37(6):1098—1114.
30. Delic S, Thuy A, Schulze M, et al. Systematic investigation of CMTM family genes suggests relevance to glioblastoma pathogenesis and CMTM1 and CMTM3 as priority targets. *Genes Chromosomes Cancer*. 2015;54(7):433—443.
31. Wu X, Hu J, Li G, et al. Biomechanical stress regulates mammalian tooth replacement via the integrin beta1-RUNX2-Wnt pathway. *EMBO J*. 2020;39(3), e102374.
32. Hong JH, Hwang ES, McManus MT, et al. TAZ, a transcriptional modulator of mesenchymal stem cell differentiation. *Science*. 2005;309(5737):1074—1078.
33. Rashdan NA, Sim AM, Cui L, et al. Osteocalcin regulates arterial calcification via altered Wnt signaling and glucose metabolism. *J Bone Miner Res*. 2020;35(2):357—367.
34. Wen Q, Jing J, Han X, et al. Runx2 regulates mouse tooth root development via activation of WNT inhibitor NOTUM. *J Bone Miner Res*. 2020;35(11):2252—2264.
35. Kirsch T, Nickel J, Sebald W. BMP-2 antagonists emerge from alterations in the low-affinity binding epitope for receptor BMPR-II. *EMBO J*. 2000;19(13):3314—3324.
36. Cong Q, Jia H, Li P, et al. p38alpha MAPK regulates proliferation and differentiation of osteoclast progenitors and bone remodeling in an aging-dependent manner. *Sci Rep*. 2017;7,e45964.
37. Sun X, Xie Z, Ma Y, et al. TGF-beta inhibits osteogenesis by upregulating the expression of ubiquitin ligase SMURF1 via MAPK-ERK signaling. *J Cell Physiol*. 2018;233(1):596—606.
38. Yang C, Liu X, Zhao K, et al. miRNA-21 promotes osteogenesis via the PTEN/PI3K/Akt/HIF-1alpha pathway and enhances bone regeneration in critical size defects. *Stem Cell Res Ther*. 2019;10(1),e65.
39. Kim JW, Oh SH, Lee MN, et al. CUEDC2 controls osteoblast differentiation and bone formation via SOCS3-STAT3 pathway. *Cell Death Dis*. 2020;11(5),e344.
40. Russo C, Ferro Y, Maurotti S, et al. Lycopene and bone: an in vitro investigation and a pilot prospective clinical study. *J Transl Med*. 2020;18(1),e43.